

**Persistence rewarded: Successful observation of the  $\tilde{B}^2\Sigma^+ + -\tilde{X}^2\Pi_g$  electronic transition of jet-cooled BS 2**

Sheng-Gui He and Dennis J. Clouthier

Citation: *The Journal of Chemical Physics* **120**, 4258 (2004); doi: 10.1063/1.1644097

View online: <http://dx.doi.org/10.1063/1.1644097>

View Table of Contents: <http://scitation.aip.org/content/aip/journal/jcp/120/9?ver=pdfcov>

Published by the [AIP Publishing](#)

---

**Articles you may be interested in**

Heavy atom nitroxyl radicals. VI. The electronic spectrum of jet-cooled H<sub>2</sub>PO, the prototypical phosphoryl free radical

*J. Chem. Phys.* **135**, 214307 (2011); 10.1063/1.3664903

The complex spectrum of a "simple" free radical: The  $\tilde{A}^1 - \tilde{X}^1$  band system of the jet-cooled boron difluoride free radical

*J. Chem. Phys.* **135**, 094305 (2011); 10.1063/1.3624528

A laser spectroscopic study of the  $\tilde{X}^1\Pi_g^2$ ,  $\tilde{A}^1\Pi_u^2$ , and  $\tilde{B}^1\Sigma_u^+ + 2$  states of B S 2 : Renner–Teller, spin-orbit, and K-resonance effects

*J. Chem. Phys.* **122**, 194314 (2005); 10.1063/1.1898221

The laser-induced fluorescence spectrum, Renner–Teller effect, and molecular quantum beats in the  $\tilde{A}^2\Pi_i - \tilde{X}^2\Pi_i$  transition of the jet-cooled HCCSe free radical

*J. Chem. Phys.* **121**, 5801 (2004); 10.1063/1.1786924

The first observation of the rhodium monofluoride molecule: Jet-cooled laser spectroscopic studies

*J. Chem. Phys.* **121**, 2591 (2004); 10.1063/1.1767036

---



# Persistence rewarded: Successful observation of the $\tilde{B}^2\Sigma_u^+ - \tilde{X}^2\Pi_g$ electronic transition of jet-cooled $\text{BS}_2$

Sheng-Gui He and Dennis J. Clouthier<sup>a)</sup>

Department of Chemistry, University of Kentucky, Lexington, Kentucky 40506-0055

(Received 6 November 2003; accepted 4 December 2003)

The  $\tilde{B} - \tilde{X}$  electronic transition of jet-cooled  $\text{BS}_2$  has been observed using laser-induced fluorescence techniques. The boron disulfide radical was produced in a pulsed electric discharge jet using a mixture of  $\text{BCl}_3$  and  $\text{CS}_2$  in high-pressure argon as the precursor. The spectrum consists of a strong  $0_0^0$  band with the  $^2\Sigma - ^2\Pi_{3/2}$  component at  $24\,393.2\text{ cm}^{-1}$  and short progressions in the symmetric stretching ( $\nu'_1 = 506.7\text{ cm}^{-1}$ ) and bending ( $\nu'_2 = 303.2\text{ cm}^{-1}$ ) modes. A rotational analysis of both spin-orbit components of the  $0_0^0$  band gave an upper state  $B$  value of  $0.093\,277\,9(19)\text{ cm}^{-1}$  and a ground-state spin-orbit coupling constant of  $A = -405.163(4)\text{ cm}^{-1}$ . The ground-state bond length of  $1.6649(2)\text{ \AA}$  increases to  $1.6812(1)\text{ \AA}$  on  $\sigma_u \rightarrow \pi_g$  electronic excitation. The  $\tilde{B} - \tilde{X}$  data have been used to further refine the Renner-Teller analysis, which is in good agreement with our previous work [J. Chem. Phys. **119**, 2047 (2003)]. © 2004 American Institute of Physics. [DOI: 10.1063/1.1644097]

## I. INTRODUCTION

Boron disulfide is the least studied of a series of isoelectronic 15 valence electron radicals ( $\text{BO}_2$ ,  $\text{CO}_2^+$ ,  $\text{NCO}$ ,  $\text{NCS}$ ) which all have  $^2\Pi$  ground states that exhibit a significant Renner-Teller effect. A variety of low-resolution studies have shown that  $\text{BS}_2$  has two electronic band systems in the UV-visible range.<sup>1-3</sup> An extensive, vibrationally, and rotationally discrete band system in the 720–500-nm region has been shown to be due to the  $\tilde{A}^2\Pi_u - \tilde{X}^2\Pi_g$  transition.<sup>3,4</sup> A further group of three bands near 410 nm has been assigned to the  $\tilde{B}^2\Sigma_u^+ - \tilde{X}^2\Pi_g$  electronic transition,<sup>1-3</sup> although no rotational analysis has previously been reported.

The  $\tilde{A} - \tilde{X}$  band system was thoroughly studied in matrices by Brom and Weltner<sup>3</sup> in 1973.  $\text{BS}_2$  was produced by vaporizing zinc sulfide and boron mixtures at high temperatures and trapping the products in neon matrices at 4 K. Their analysis identified the  $0_0^0$  band at  $13\,766\text{ cm}^{-1}$  and led to the conclusion that there was little or no Renner-Teller effect in the upper  $^2\Pi_u$  electronic state. Taking advantage of the weakly allowed  $^2\Pi_{1/2} - ^2\Pi_{3/2}$  bands observed in the matrix, they obtained ground- and  $\tilde{A}$ -state spin-orbit splittings of  $-440\text{ cm}^{-1}$  and  $-263\text{ cm}^{-1}$ , with vibrational frequencies of  $\nu''_1 = 510\text{ cm}^{-1}$ ,  $\nu''_2 \sim 120\text{ cm}^{-1}$ , and  $\nu''_3 = 1015\text{ cm}^{-1}$  and  $\nu'_1 = 506\text{ cm}^{-1}$ ,  $\nu'_2 = 311\text{ cm}^{-1}$ , and  $\nu'_3 = 1535\text{ cm}^{-1}$ .

Recently,<sup>4</sup> we obtained the first electronic spectra of jet-cooled  $\text{BS}_2$ , using the pulsed discharge technique with a gaseous mixture of  $\text{BCl}_3$  and  $\text{CS}_2$  in high-pressure argon as the precursor. The  $\tilde{A}^2\Pi_u - \tilde{X}^2\Pi_g$  electronic band system was studied by a combination of laser-induced fluorescence (LIF) and wavelength-resolved emission techniques. A long progression of strong bands involving the  $\nu'_1$  (B–S stretching) mode and combinations involving  $2\nu'_2$  and  $2\nu'_3$ , as well as

many hot bands built on the  $2_1^1$  band, were assigned in the LIF spectrum. Due to the restrictive  $\Delta P = 0$  selection rule, the spin-orbit splittings could not be measured directly for these parallel transitions. Instead, the upper-state spin-orbit parameter was obtained indirectly, through the variation of the energy level splittings as a function of the vibrational quantum numbers, by fitting excited-state vibrational combination differences. Subsequently, the ground-state spin-orbit splitting was obtained by rotational analysis of the  $0_0^0$  band with the upper-state splitting fixed at the value obtained from the vibrational analysis. Vibrational and rotational analysis showed that the ground state exhibits a substantial Renner-Teller effect with  $\epsilon = -0.2012(34)$  and a zero-point level spin-orbit coupling constant of  $A_0 = -404.683(3)\text{ cm}^{-1}$ . Angular momentum coupling is negligible in the excited state, which has a much smaller spin-orbit coupling constant of  $A_0 = -259.15(12)\text{ cm}^{-1}$ , in agreement with the previous matrix work. The  $^{11}\text{BS}_2$  vibrational frequencies are  $\omega''_1 = 542.8$ ,  $\omega''_2 = 285.0$ ,  $\omega''_3 = 1010.5$ ,  $\omega'_1 = 514.1$ ,  $\omega'_2 = 309.7$ , and  $\omega'_3 = 1543.6\text{ cm}^{-1}$ . High-resolution spectra of the  $0_0^0$  band of  $^{11}\text{BS}_2$  were rotationally analyzed to obtain effective molecular structures of  $r''_0(\text{BS}) = 1.6648(4)\text{ \AA}$  and  $r'_0(\text{BS}) = 1.7127(5)\text{ \AA}$ . The spectroscopic data clearly establish that the radical has the linear SBS structure in both combining state. *Ab initio* methods were used to predict the  $\text{BS}_2$  spectroscopic parameters and good agreement with experiment was found. Several attempts to observe the 415-nm  $\tilde{B} - \tilde{X}$  band system of jet-cooled  $\text{BS}_2$  using LIF techniques were unsuccessful, suggesting that the  $\tilde{B}$  state has a low quantum yield of fluorescence, although this is unlikely for such a small molecule.

Believing in the old adage that *if at first you don't succeed, try, try, try again*, we persisted in attempts to observe the  $\tilde{B} - \tilde{X}$  transition and have finally succeeded in doing so, as we report in this work. By simultaneous rotational analy-

<sup>a)</sup> Author to whom correspondence should be addressed.

sis of both spin-orbit components we have obtained a direct and precise measure of the ground-state spin-orbit splitting and have derived the effective excited-state molecular structure. These results have been further used to refine the molecular constants for the  $\tilde{X}^2\Pi_g$  state of <sup>11</sup>BS<sub>2</sub>.

## II. EXPERIMENT

In our previous study,<sup>4</sup> BS<sub>2</sub> was obtained from a gas-phase precursor mixture of 3% BCl<sub>3</sub> and 1% CS<sub>2</sub> in argon, contained in a stainless steel cylinder equipped with a regulator, which was delivered at a pressure of 40 psi into a pulsed discharge at the exit of a molecular beam valve (General Valve, series 9). Although this method gave strong spectra of the  $\tilde{A}-\tilde{X}$  band system, it did not allow us to obtain spectra of the  $\tilde{B}-\tilde{X}$  bands at 415 nm. Subsequent experimentation showed that a gas-phase mixture of 3% BCl<sub>3</sub> in argon flowed at 40 psi pressure over the surface of room-temperature, liquid CS<sub>2</sub> gave much stronger BS<sub>2</sub> spectra and permitted us to obtain LIF spectra of the UV band system. This precursor mixture was injected into a Delrin flow channel attached to the exit of the molecular beam valve. At the appropriate time in the gas pulse, a pulsed electric discharge was struck between two stainless steel ring electrodes mounted in the flow channel, which fragmented the precursor molecules and formed BS<sub>2</sub> by subsequent chemical reactions.

Low-resolution LIF spectra were obtained by crossing the supersonic expansion of the discharge products 1.5 cm downstream of the discharge apparatus with the beam of a tunable dye laser (Lumonics HD-500). The resulting fluorescence was imaged by a 5-cm-focal-length lens through an appropriate cutoff filter onto the photocathode of a high-gain photomultiplier tube (EMI 9816QB). Low-resolution (0.1 cm<sup>-1</sup>) LIF spectra were excited in the 420–390-nm range and calibrated using opticalgalvanic lines from an argon-filled hollow cathode lamp.

High-resolution (0.04 cm<sup>-1</sup>) spectra of the 0<sub>0</sub><sup>0</sup> band at 410 nm were obtained in the same discharge jet apparatus. In order to obtain laser radiation in the near ultraviolet that could be accurately wavelength calibrated, we used a variant of the Raman shifting technique previously described.<sup>5</sup> A 308-nm pumped Lambda-Physik ScanMate2E dye laser equipped with an intracavity étalon and operated with Coumarin 503 laser dye gave narrow-bandwidth (0.035 cm<sup>-1</sup>), high-energy (10–15 mJ) pulses in the 490–505-nm region. This radiation was focused into a Raman shifting cell filled with hydrogen at a pressure of 200 psi. The Raman shifted beams generated in this process were separated by a prism and the weak first anti-Stokes beam (407–417 nm) was used to excite the BS<sub>2</sub> LIF spectrum while the first Stokes beam (615–639 nm) was used to excite I<sub>2</sub> LIF spectra. The LIF and calibration spectra were recorded simultaneously with a LABVIEW-based digital data acquisition system of our design.<sup>6</sup> As the hydrogen Raman shifts can be very accurately calculated as a function of pressure,<sup>5</sup> and the iodine absorption lines have been accurately measured,<sup>7,8</sup> we were able to calibrate the BS<sub>2</sub> LIF spectra to an estimated accuracy of ±0.003 cm<sup>-1</sup>.

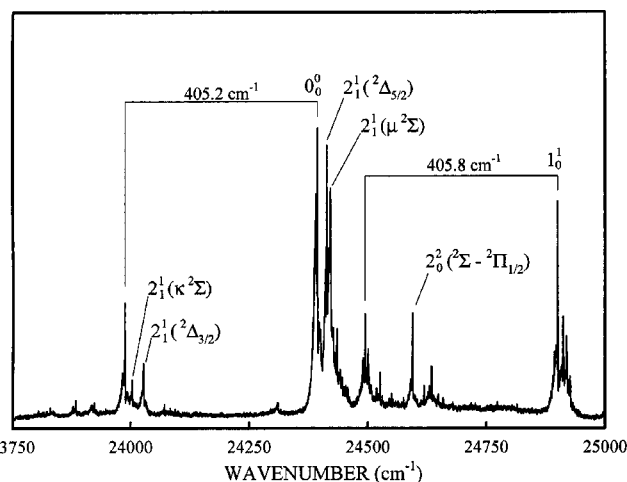


FIG. 1. Portion of the low-resolution  $\tilde{B}^2\Sigma_u^+ - \tilde{X}^2\Pi_g$  spectrum of jet-cooled BS<sub>2</sub> with the assignments of some of the stronger features. The vertical leaders denote the two spin-orbit components ( $^2\Pi_{1/2}$  on the left,  $^2\Pi_{3/2}$  on the right) of the intense 0<sub>0</sub><sup>0</sup> and 1<sub>0</sub><sup>1</sup> bands. All four components of the 2<sub>1</sub><sup>1</sup> sequence band are identified, with the lower-state symmetries in parentheses, along with the  $^2\Sigma - ^2\Pi_{1/2}$  component of the 2<sub>0</sub><sup>2</sup> band.

## III. RESULTS AND ANALYSIS

The ground-state electron configuration of linear BS<sub>2</sub> is  $\dots(\sigma_g)^2(\sigma_u)^2(\pi_u)^4(\pi_g)^3\tilde{X}^2\Pi_g$  (inverted), with excited states  $\dots(\sigma_g)^2(\sigma_u)^2(\pi_u)^3(\pi_g)^4\tilde{A}^2\Pi_u$  (inverted) and  $\dots(\sigma_g)^2(\sigma_u)^1(\pi_u)^4(\pi_g)^4\tilde{B}^2\Sigma_u^+$ . The  $\sigma_u$  and  $\pi_u$  orbitals are bonding and the  $\pi_g$  orbitals are essentially pure  $3p\pi$  nonbonding orbitals on the sulfur atoms. The vibrational frequencies are conventionally labeled as  $\nu_1$  ( $\sigma_g$ , symmetric BS stretch),  $\nu_2$  ( $\pi_{g,u}$ , bend), and  $\nu_3$  ( $\sigma_u$ , antisymmetric BS stretch). The vibronic selection rules are  $\Delta v_1 = 0, \pm 1, \pm 2, \dots$  and  $\Delta v_2$  or  $\Delta v_3 = 0, \pm 2, \dots$  and transitions from both spin-orbit components of the zero-point level of the ground state are allowed for the  $\tilde{B}^2\Sigma_u^+ - \tilde{X}^2\Pi_g$  electronic transition.

A portion of the low-resolution LIF spectrum of the  $\tilde{B}-\tilde{X}$  transition of BS<sub>2</sub> is shown in Fig. 1. The spectrum is dominated by an intense band at 24 393.2 cm<sup>-1</sup>, which is readily assigned as the  $^2\Sigma - ^2\Pi_{3/2}$  component of the 0<sub>0</sub><sup>0</sup> band; the corresponding  $^2\Sigma - ^2\Pi_{1/2}$  component occurs at 23 988.0 cm<sup>-1</sup>, giving a ground-state spin-orbit splitting of -405.2 cm<sup>-1</sup>, in agreement with the -404.7 cm<sup>-1</sup> value obtained previously.<sup>4</sup> We assign the major cold band features in the spectrum to a short progression ( $1_0^n, n=0-2$ ) involving the excited-state symmetric stretch, with a fundamental frequency of  $\nu_1' = 506.7$  cm<sup>-1</sup>. This assignment is in accordance with the conclusions of Brom and Weltner,<sup>3</sup> allowing for an approximately -100 cm<sup>-1</sup> matrix shift. We also detected weak bands at 24 999.0 and 25 039.5 cm<sup>-1</sup>, not found in previous studies, which we assign as two components of the 2<sub>0</sub><sup>2</sup> band, originating from the  $^2\Pi_{3/2}$  level. The corresponding transitions from the upper spin-orbit component ( $^2\Pi_{1/2}$ ) were also identified and the pattern of transitions is repeated for the 1<sub>0</sub><sup>1</sup>2<sub>0</sub><sup>2</sup> band.

The remaining bands in the spectrum were readily assigned as hot bands, based on our previous Renner-Teller analysis of the ground state.<sup>4</sup> All four components of the 2<sub>1</sub><sup>1</sup>

TABLE I. LIF bands observed in the  $\tilde{B}^2\Sigma_u^+ - \tilde{X}^2\Pi_g$  spectrum of jet-cooled  $^{11}\text{BS}_2$ .

Assignment	Maximum (cm <sup>-1</sup> )	Assignment	Maximum (cm <sup>-1</sup> )
$2_0^0(^2\Sigma - \mu^2\Pi_{3/2})$	23804.0	$1_0^1 2_1^1(^2\Pi - ^2\Delta_{3/2})$	24525.5
$2_0^0(^2\Sigma - \mu^2\Pi_{1/2})$	23828.9	$2_0^2(^2\Sigma - ^2\Pi_{1/2})$	24594.0 <sup>a</sup>
$1_1^0(^2\Sigma - ^2\Pi_{3/2})$	23883.5	$2_0^2(^2\Delta - ^2\Pi_{1/2})$	24634.5 <sup>a</sup>
$1_0^1 2_1^1(^2\Pi - \mu^2\Sigma)$	23917.6	$1_0^1(^2\Sigma - ^2\Pi_{3/2})$	24899.9
$1_0^1 2_1^1(^2\Pi - ^2\Delta_{5/2})$	23923.6	$1_0^1 2_1^1(^2\Pi - ^2\Delta_{5/2})$	24911.4
$0_0^0(^2\Sigma - ^2\Pi_{1/2})$	23988.0	$1_0^1 2_1^1(^2\Pi - \mu^2\Sigma)$	24918.3
$2_1^1(^2\Pi - \kappa^2\Sigma)$	24003.5	$1_0^1 2_0^2(^2\Sigma - \mu^2\Pi_{1/2})$	24927.3
$2_1^1(^2\Pi - ^2\Delta_{3/2})$	24027.2	$2_0^2(^2\Sigma - ^2\Pi_{3/2})$	24999.0
$1_0^1 2_0^2(^2\Sigma - \mu^2\Pi_{3/2})$	24310.8	$1_0^1(^2\Sigma - ^2\Pi_{1/2})$	24999.0
$0_0^0(^2\Sigma - ^2\Pi_{3/2})$	24393.2	$2_0^2(^2\Delta - ^2\Pi_{3/2})$	25039.5
$2_1^1(^2\Pi - ^2\Delta_{5/2})$	24413.1	$1_0^1 2_0^2(^2\Sigma - ^2\Pi_{1/2})$	25086.3
$2_1^1(^2\Pi - \mu^2\Sigma)$	24420.2	$1_0^1 2_0^2(^2\Delta - ^2\Pi_{1/2})$	25120.5 <sup>?</sup>
$2_2^2(^2\Sigma - \mu^2\Pi_{1/2})$	24435.4	$1_0^1(^2\Sigma - ^2\Pi_{3/2})$	25404.1
$1_0^1 2_0^2(^2\Sigma - ^2\Pi_{3/2})$	24489.8	$1_0^1 2_1^1(^2\Pi - ^2\Delta_{5/2})$	25407.7
$1_0^1(^2\Sigma - ^2\Pi_{1/2})$	24494.1	$1_0^1 2_0^2(^2\Sigma - ^2\Pi_{3/2})$	25492.5
$1_0^1 2_1^1(^2\Pi - \kappa^2\Sigma)$	24501.7		

<sup>a</sup>The following  $^{10}\text{BS}_2$  isotope bands were assigned:  $2_0^2(^2\Sigma - ^2\Pi_{1/2})$  at 24 618.9 cm<sup>-1</sup> and  $2_0^2(^2\Delta - ^2\Pi_{1/2})$  at 24 658.8 cm<sup>-1</sup>.

sequence band are readily apparent as shown in Fig. 1, consistent with our previous studies that showed substantial population of  $v_2''=1$  in the discharge jet expansion. This pattern of four features is repeated for the  $1_0^1 2_1^1$  hot band and the  $^2\Delta_{5/2}$  component was found for the  $1_0^1 2_1^1$  band. The  $1_1^0$ ,  $1_1^0 2_1^1$ , and  $1_0^1 2_0^2$  hot bands were also assigned, giving a ground-state symmetric stretching frequency, uncorrected for Fermi resonance, of 509.7 cm<sup>-1</sup>. Finally, five very weak bands were assigned as transitions from  $v_2''=2$  to the various upper-state levels identified from the strong cold bands. The vibrational assignments are summarized in Table I.

We have recorded both spin-orbit components of the  $\tilde{B} - \tilde{X} 0_0^0$  band of  $^{11}\text{BS}_2$  at high resolution; the stronger  $^2\Sigma - ^2\Pi_{3/2}$  band is shown in Fig. 2. Four of the six branches of the band have been resolved at our resolution of 0.04 cm<sup>-1</sup>—the  $R_{11}$  and  $Q_{21}$  branches are blended together forming the strong unresolved feature near the band center. Both

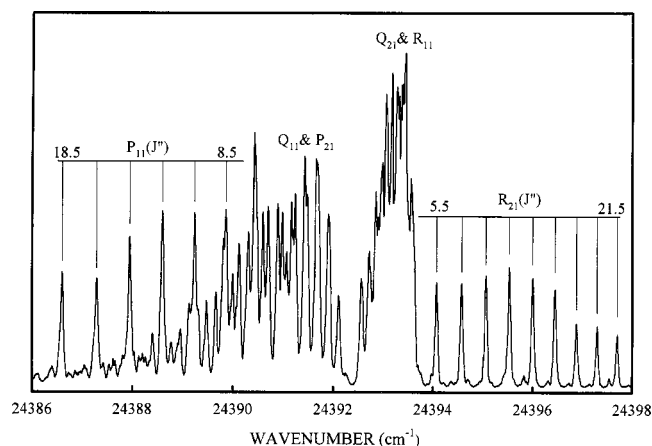


FIG. 2. High-resolution spectrum of the  $^2\Sigma - ^2\Pi_{3/2}$  component of the  $0_0^0$  band of the  $\tilde{B}^2\Sigma_u^+ - \tilde{X}^2\Pi_g$  system of  $\text{BS}_2$  showing the various branches and some of the rotational assignments.

TABLE II. Molecular constants (in cm<sup>-1</sup>) for the vibrational zero-point levels of the known electronic states of  $^{11}\text{BS}_2$ .

Parameter	$\tilde{X}^2\Pi_i$	$\tilde{A}^2\Pi_i$	$\tilde{B}^2\Sigma_u^+$
$B$	0.095105 <sub>3</sub> (25) <sup>a</sup>	0.0898546(81)	0.0932779(19)
$A_0$	-405.163 <sub>7</sub> (4)	-259.631 <sub>0</sub> (2)	—
$\gamma$	—	—	0.00742 <sub>9</sub> (10)
$10^4 A_d$	-0.87 <sub>2</sub> (14)	0.0 <sup>b</sup>	—
$10^2(p+2q)$	0.250(25)	0.508(29)	—
$T_0$	0.0	13839.391 <sub>9</sub> (2)	24189.533 <sub>7</sub> (2)
$\#^c$	135	87	87
$\sigma$ (cm <sup>-1</sup> ) <sup>d</sup>	0.0045	0.0033	0.0037

<sup>a</sup>The numbers in parentheses are  $3\sigma$  error limits and are right justified to the last digit on the line; sufficient additional digits are quoted to reproduce the original data to full accuracy.

<sup>b</sup>Parameter fixed in the final least-squares analysis.

<sup>c</sup>Number of combination differences or transitions fitted.

<sup>d</sup>Overall standard deviation of fit.

components of the band were readily assigned as branches of a  $^2\Sigma - ^2\Pi_i$  vibronic band with Hund's case (a) coupling in the lower state and Hund's case (b) coupling in the upper state. The sulfur atoms have zero nuclear spin and the nuclear statistical weights are such that alternate  $\Lambda$ -doubling levels are missing, so that only one level exists for each  $J$  value. This leads to a staggering in the appearance of some of the branches in the  $^2\Sigma - ^2\Pi_{1/2}$  component.

Although the  $\tilde{B} - \tilde{X} 0_0^0$  band could be satisfactorily fitted by itself, we elected to include data from the  $\tilde{A} - \tilde{X} 0_0^0$  band as well, in order to obtain the best set of molecular constants and improve on the assumptions made in our earlier analysis,<sup>4</sup> where no direct measure of the spin-orbit splittings in the  $\tilde{X}$  and  $\tilde{A}$  states was possible. First, for each band, including both spin components, a data set of strong, symmetric, unblended lines was chosen and all possible ground-state combination differences were formed. The ground-state constants were refined by fitting the combination differences to the lower-state  $^2\Pi_i$  effective Hamiltonian in the  $R^2$  formulation using the matrix elements tabulated previously.<sup>9</sup> This gave the ground-state constants summarized in Table II, which are in generally good agreement with those obtained previously.<sup>4</sup> The only substantial difference is in the  $\Lambda$ -doubling constant  $p+2q$ , which is smaller than previously determined. This difference can be traced to a substantial correlation between the  $\tilde{X}$ - and  $\tilde{A}$ -state  $\Lambda$ -doubling constants obtained from the previous analysis of the  $\tilde{A} - \tilde{X} 0_0^0$  band. It is especially gratifying that the present spin-orbit coupling constant  $A_0 = -405.164(4)$  cm<sup>-1</sup> agrees so well with the  $-404.683(3)$  value determined previously by fixing the upper-state spin-orbit interval at the value obtained from the Renner-Teller analysis.

Subsequently, the  $\tilde{A}$ - and  $\tilde{B}$ -state molecular constants were determined by fitting the  $0_0^0$  band transition frequencies, with the ground-state constants fixed at the values given in Table II. The  $\tilde{A}$ -state Hamiltonian was the same as that of the ground state, whereas the  $\tilde{B}$ -state energy levels were modeled using only the band origin  $T_0$ , the rotational constant  $B$ , and the spin-rotation coupling constant  $\gamma$  contained in the  $^2\Sigma^+$  energy level expressions given in Eqs. (1) and (2)

TABLE III. Vibrational parameters (in cm<sup>-1</sup>) for the ground state of <sup>11</sup>BS<sub>2</sub>.

Parameter	$\tilde{X}^2\Pi_g$	
	Present	Previous <sup>a</sup>
$\omega_1$	544.80 <sub>6</sub> (47) <sup>b</sup>	542.76 <sub>7</sub> (61) <sup>b</sup>
$\omega_2$	283.54 <sub>9</sub> (27)	284.96 <sub>2</sub> (46)
$\omega_3$	1010.7 <sub>18</sub> (15)	1010.5 <sub>10</sub> (11)
$A$	-414.41 <sub>6</sub> (23)	-413.80 <sub>2</sub> (74)
$\epsilon$	-0.2098(17)	-0.2012(34)
$g_4$	2.933 <sub>7</sub> (39)	2.785 <sub>4</sub> (54)
$g_K$	0.82 <sub>8</sub> (13)	—
$W_1$	19.232 <sub>2</sub> (72)	19.020 <sub>2</sub> (88)
$W_2$	1.00 <sub>6</sub> (8)	1.03 <sub>1</sub> (11)
$x_{13}$	-8.09 <sub>8</sub> (116)	-7.82 <sub>9</sub> (89)
$x_{23}$	-1.88 <sub>6</sub> (66)	-1.85 <sub>3</sub> (51)
$x_{33}$	6.21 <sub>8</sub> (42)	6.24 <sub>4</sub> (34)

<sup>a</sup>Reference 4.<sup>b</sup>The numbers in parentheses are 1 $\sigma$  error limits and are right justified to the last digit on the line; sufficient additional digits are quoted to reproduce the original data to full accuracy.<sup>c</sup>The  $A$  values in Tables II and III are different. In the Renner–Teller analysis the spin–orbit coupling constant is defined by  $A_{\text{eff}}=A[1-\frac{1}{8}\epsilon^2K(K+1)]$  for the unique levels so that the variation with  $K$  is included explicitly in the model whereas in Table II it is  $A_{\nu=0}$ , obtained from the rotational analysis, which is quoted.

of Ref. 9. The constants are collected in Table II. The  $\tilde{A}$ -state values are in good agreement with those obtained in the previous work.<sup>4</sup>

Our precise determination of the ground-state spin–orbit splitting and the new ground-state vibrational combination differences available from the hot bands in Table I have permitted us to refine the BS<sub>2</sub> ground-state Renner–Teller analysis. In particular, the  $\tilde{B}-\tilde{X}^2\Pi_g$  hot bands allowed direct determination of the relative energies of the four levels of  $\nu_2''$  as  $\mu^2\Sigma=0.0$ ,  ${}^2\Delta_{5/2}=6.7\text{ cm}^{-1}$ ,  ${}^2\Delta_{3/2}=393.7\text{ cm}^{-1}$ , and  $\kappa^2\Sigma=417.0\text{ cm}^{-1}$ , which made it possible to determine the  $g_K$  parameter. We have used the Renner–Teller model described previously<sup>4</sup> in a weighted least-squares analysis to fit a total of 89 combination differences obtained from the  $\tilde{B}-\tilde{X}$  LIF spectra and previously studied  $\tilde{A}-\tilde{X}$  emission spectra to an overall weighted standard deviation of 2.03 cm<sup>-1</sup>. The resulting constants are given in Table III, along with previously determined values. Both sets of parameters are in general agreement, although there are some noticeable changes

due to the inclusion of  $g_K$  and the refined value of the spin–orbit splittings in the model. Using the  $\tilde{B}-\tilde{X}^2\Pi_g$  band transition frequencies and the lower-state bending mode energy from the Renner–Teller analysis, we calculate the excited-state bending frequency to be 303.2 cm<sup>-1</sup>, only slightly larger than half the  $2\nu_2'$  interval of 605.8 cm<sup>-1</sup>.

#### IV. AB INITIO CALCULATIONS

We have used *ab initio* theory to predict the molecular properties of BS<sub>2</sub> in the various electronic states to see how well they agree with the experimental data. The GAUSSIAN 98 programs<sup>10</sup> were used in conjunction with a variety of levels of theory and a range of basis sets to calculate the bond length, vibrational frequencies, and energies of the three observed electronic states of <sup>11</sup>BS<sub>2</sub>. In general, density functional theory (B3LYP) with Dunning's correlation-consistent basis sets augmented by diffuse functions (aug-cc-pVTZ and aug-cc-pVQZ) (Ref. 11) gave reasonable agreement with experiment, but the best results were obtained with coupled cluster theory and only these are reported in this work, as summarized in Table IV.

#### V. DISCUSSION

This work reports the vibrational and rotational analysis of the  $\tilde{B}^2\Sigma_u^+-\tilde{X}^2\Pi_g$  band system of boron disulfide in the blue region of the spectrum. We have clearly established by rotational analysis that the molecule is linear in both the ground and excited states. The vibrational analysis of the  $\tilde{B}^2\Sigma_u^+-\tilde{X}^2\Pi_g$  bands of BS<sub>2</sub> is unequivocal and is supported by a variety of ancillary lines of evidence. The only bands which exhibit assignable <sup>10</sup>BS<sub>2</sub> features are two components of  $2^2_0$ , as documented in the footnote to Table I. Theory gives the isotope effect as<sup>12</sup>

$$\frac{\omega_3(^{10}\text{BS}_2)}{\omega_3(^{11}\text{BS}_2)} = \frac{\omega_2(^{10}\text{BS}_2)}{\omega_2(^{11}\text{BS}_2)} = \sqrt{\frac{1+2m_S/m(^{10}\text{B})}{1+2m_S/m(^{11}\text{B})}} = 1.04158, \quad (1)$$

while experiment gives a  $2\nu_2'$  ratio (assuming negligible  $0_0^0$  band isotope effect) of 1.041 for the  ${}^2\Sigma$  component. The upper-state vibrational frequencies calculated at the CCSD(T)/aug-cc-pVTZ level of theory (Table IV) are also in excellent agreement with the values of  $\nu_1'$  and  $\nu_2'$  derived from experiment. The rotational analysis shows that the as-

TABLE IV. Vibrational parameters (in cm<sup>-1</sup>), bond lengths (Å), and energies (cm<sup>-1</sup>) for the ground and electronic excited states of <sup>11</sup>BS<sub>2</sub>.

Parameter	$\tilde{X}^2\Pi_g$		$\tilde{A}^2\Pi_u$		$\tilde{B}^2\Sigma_u^+$	
	Experiment <sup>a,c</sup>	<i>Ab initio</i> <sup>b</sup>	Experiment <sup>c</sup>	<i>Ab initio</i> <sup>b</sup>	Experiment <sup>a,d</sup>	<i>Ab initio</i> <sup>b</sup>
$\omega_1$	544.8	550.4	514.1	514.4	506.7	516.6
$\omega_2$	283.5	282.7	309.7	316.8	303.2	299.0
$\omega_3$	1010.7	944.1	1543.6	1569.7	—	1052.0
$r_0$	1.6649	1.671	1.7129	1.718	1.6812	1.687
$T_0$	0.0	0.0	13839.392	14269	24189.534	24148

<sup>a</sup>This work.<sup>b</sup>CCSD(T)/aug-cc-pVQZ calculations, frequencies with aug-cc-pVTZ basis set.<sup>c</sup>Reference 4.<sup>d</sup>The  $\tilde{B}$ -state vibrational frequencies are the fundamental rather than the harmonic frequencies.

signed  $0_0^0$  band does originate from the same vibrational level of the ground state as the  $0_0^0$  band of the  $\tilde{A}-\tilde{X}$  transition. The pattern of hot bands substantiates the cold band assignments and the lower-state intervals are in accordance with those derived in our previous Renner–Teller analysis of the ground state.

It is apparent from Fig. 2 that there are no  $^{10}\text{BS}_2$  spectral lines evident in the high-resolution spectrum of the  $0_0^0$  band. A calculation using the known ground- and  $\tilde{B}$  excited-state  $^{11}\text{BS}_2$  vibrational frequencies and the *ab initio* value for  $\nu_3'$  along with the theoretical isotope ratio in Eq. (1) gives a  $0_0^0$  band isotope shift ( $^{10}\text{BS}_2-^{11}\text{BS}_2$ ) of  $\sim 1.2\text{ cm}^{-1}$ . Since the  $B$  values are the same in both isotopomers and the rotational spacings are of the order of  $0.5\text{ cm}^{-1}$ , the rotational lines of  $^{11}\text{BS}_2$  and  $^{10}\text{BS}_2$  must be accidentally coincident, although shifted by one or two units of the angular momentum quantum number  $J$ . This also accounts for the broader than expected width of the overlapping  $Q_{21}$  and  $R_{11}$  branch feature.

The effective ( $r_0$ ) B–S bond lengths calculated from the rotational constants are  $\tilde{X}=1.6649(2)\text{ \AA}$ ,  $\tilde{A}=1.7129(1)\text{ \AA}$ , and  $\tilde{B}=1.6812(1)\text{ \AA}$ . The bond length changes are as expected from qualitative molecular orbital theory. Excitation of an electron from the bonding  $\pi_u$  orbitals to the partially filled nonbonding  $\pi_g$  orbitals ( $\tilde{A}-\tilde{X}$  transition) elongates the bond by  $0.048\text{ \AA}$ , whereas promotion of an electron from the slightly bonding  $\sigma_u$  orbital to the  $\pi_g$  orbitals ( $\tilde{B}-\tilde{X}$  transition) only increases the bond length by  $0.016\text{ \AA}$ . The Franck–Condon activity in the  $\tilde{B}-\tilde{X}$  spectrum, with most of the intensity concentrated in the  $0_0^0$  band, is entirely consistent with the small structural change in electronic excitation.

Coupled cluster theory with large basis sets does an excellent job of predicting the molecular properties of  $\text{BS}_2$ , as shown in Table IV. Theory consistently slightly overestimates the bond lengths, although they are all within  $0.006\text{ \AA}$

of the experimental  $r_0$  values. The calculated vibrational frequencies differ from experiment, where available, by a maximum of 6.6%, although the majority of the differences are below 2%. The zero-point-corrected electronic excitation energies differ from experiment by  $430\text{ cm}^{-1}$  ( $\tilde{A}-\tilde{X}$ ) and  $-41\text{ cm}^{-1}$  ( $\tilde{B}-\tilde{X}$ ), which is very good agreement.

The present analysis confirms all aspects of our previous Renner–Teller analysis<sup>4</sup> of the ground state of  $^{11}\text{BS}_2$ . The data in Table III show that the vibrational parameters change only slightly when the more precise zero-point spin–orbit splitting and lower-bending-level intervals are included in the least-squares analysis.

## ACKNOWLEDGMENTS

The authors thank Brandon Tackett for assistance in operating the instrumentation and Dr. Corey Evans for early attempts to observe the spectrum. This research was supported by the National Science Foundation.

<sup>1</sup>V. A. Koryazhkin and A. A. Mal'tsev, *Vestn. Mosk. Univ., Ser. 2: Khim.* **21**, 6 (1966).

<sup>2</sup>A. G. Briggs and R. E. Simmons, *Spectrosc. Lett.* **19**, 953 (1986).

<sup>3</sup>J. M. Brom, Jr. and W. Weltner, Jr., *J. Mol. Spectrosc.* **45**, 82 (1973).

<sup>4</sup>S. G. He, C. J. Evans, and D. J. Clouthier, *J. Chem. Phys.* **119**, 2047 (2003), and references therein.

<sup>5</sup>J. Karolczak and D. J. Clouthier, *Rev. Sci. Instrum.* **61**, 1607 (1990).

<sup>6</sup>R. H. Judge and D. J. Clouthier (unpublished).

<sup>7</sup>S. Gerstenkorn and P. Luc, *Atlas du Spectre D'Absorption de la Molecule d'Iode* (Editions du C.N.R.S., Paris, 1978).

<sup>8</sup>S. Gerstenkorn and P. Luc, *Rev. Phys. Appl.* **14**, 791 (1979).

<sup>9</sup>T. C. Smith, H. Li, D. J. Clouthier, C. T. Kingston, and A. J. Merer, *J. Chem. Phys.* **112**, 3662 (2000).

<sup>10</sup>M. J. Frisch *et al.*, computer code GAUSSIAN 98, revision A.11, Gaussian, Inc., Pittsburgh, PA, 1998.

<sup>11</sup>T. H. Dunning, Jr., *J. Chem. Phys.* **90**, 1007 (1989).

<sup>12</sup>G. Herzberg, *Molecular Spectra and Molecular Structure II. Infrared and Raman Spectra of Polyatomic Molecules* (Van Nostrand, New York, 1945), p. 230.